Synthesis of novel 1,2-benzothiazine 1,1-dioxide-3-ethanone oxime N-aryl acetamide ether derivatives as potent anti-inflammatory agents and inhibitors of monocyte-to-macrophage tra...

ARTICLE *in* EUROPEAN JOURNAL OF MEDICINAL CHEMISTRY · MARCH 2014

Impact Factor: 3.45 · DOI: 10.1016/j.ejmech.2013.12.053

8 AUTHORS, INCLUDING:

Mallareddy Gannarapu
Indian Institute of Chemical Technology
14 PUBLICATIONS **21** CITATIONS
SEE PROFILE

Sathish Babu
Indian Institute of Chemical Technology
9 PUBLICATIONS **21** CITATIONS
SEE PROFILE

Punna Nagender
Indian Institute of Chemical Technology
14 PUBLICATIONS **22** CITATIONS
SEE PROFILE

Srigiridhar Kotamraju
Indian Institute of Chemical Technology
74 PUBLICATIONS **2,482** CITATIONS
SEE PROFILE

European Journal of Medicinal Chemistry 75 (2014) 143–150

Contents lists available at ScienceDirect

European Journal of Medicinal Chemistry

journal homepage: http://www.elsevier.com/locate/ejmech

Original article

Synthesis of novel 1,2-benzothiazine 1,1-dioxide-3-ethanone oxime *N*-aryl acetamide ether derivatives as potent anti-inflammatory agents and inhibitors of monocyte-to-macrophage transformation

Malla Reddy Gannarapu [a], Sathish Babu Vasamsetti [b], Nagender Punna [a], Naresh Kumar Royya [a], Shanthan Rao Pamulaparthy [a], Jagadeesh Babu Nanubolu [c], Srigiridhar Kotamraju [b,*], Narsaiah Banda [a,*]

[a] Fluoroorganic Division, CSIR-Indian Institute of Chemical Technology, Tarnaka, Hyderabad 500607, India
[b] Centre for Chemical Biology, CSIR-Indian Institute of Chemical Technology, Tarnaka, Hyderabad 500607, India
[c] Centre for X-ray Crystallography, CSIR-Indian Institute of Chemical Technology, Tarnaka, Hyderabad 500607, India

ARTICLE INFO

Article history:
Received 21 August 2013
Received in revised form
18 November 2013
Accepted 25 December 2013
Available online 8 January 2014

Keywords:
N-aryl acetamide
Oxime ether
Anti-inflammatory activity
PMA-phorbol 12-myristate 13-acetate

ABSTRACT

A series of novel 1,2-benzothiazine 1,1-dioxide-3-ethanone oxime *N*-aryl acetamide ether derivatives **7a**–**h** and **9a**–**h** were synthesized starting from sodium salt of saccharin **1** in series of steps. Final compounds **7a**–**h** and **9a**–**h** were evaluated for the anti-inflammatory activity and their ability to inhibit monocyte-to-macrophage transformation. Compounds **7e**, **9b**, **9e** and **9h** showed impressive anti-inflammatory activities (TNF-α, IL-8 and MCP-1) at micro molar concentration which was found to be better than positive control i.e., piroxicam. Compound **9e** marginally and compound **9h** significantly inhibited PMA-induced MMP-9 gelatinase activity. Also compounds **9e** and **9h** greatly inhibited the PMA-induced monocyte-to-macrophage transformation, a pre-requisite step in the formation of atheroma.

1. Introduction

Inflammation is a multi-factorial process involved in many pathological disorders. In response to infection stimulus, endothelial activation and metabolic disorders like diabetes myeloid lineage cells activate and generate an inflammatory environment by secreting many pro-inflammatory cytokines like interleukins, tumor necrosis factor-α (TNF-α), chemokines etc. The TNF-α is produced mainly by macrophages and T-cells play a key role in many physiological immune processes. Over activation of TNF-α is correlated with a plethora of pathological conditions including diabetes [1], atherosclerosis [2], multiple sclerosis [3], ulcerative colitis [4], stroke [5] and cirrhosis [6]. There is a spectrum of drugs currently available to inhibit TNF-α such as Etanercept, Infliximab and Adalimumab, however they have been shown to cause adverse side effects such as aplastic anaemia, pancytopenia, vasculitis and congestive heart failure [7] with limitation of oral bio-availability, potential antigenicity and low tissue penetrating capability. Though several efforts have been made on synthesis of new molecules to inhibit/regulate TNF-α, no small molecules have been approved as reliable inhibitors till now.

The human chemokine Interleukin-8 (IL-8) in particular, a member of the CXC chemokine family produced by stimulated monocytes [8], activates adhesion molecules expression on endothelial cells [9] and also serves as an important activator and chemoattractant for neutrophils [10], as well as T-cells [11]. Monocyte chemoattractant protein-1 (MCP-1) levels are known to be elevated in various disorders including rheumatoid arthritis, insulin-resistant diabetes etc. [12,and13]. Higher levels of MCP-1 are reported in patients with coronary lesions compared to patients with normal coronary arteries (NCA) [14]. MCP-1 also contributes to atherosclerosis by attracting monocytes into the sub-endothelium, a key event in the process of atherogenesis [15].

Matrix metalloproteinases (MMPs) are large family of proteases that degrade extracellular matrix, play a pivotal role in several disorders including cancer by promoting invasion and metastasis of tumors [16]. MMPs are highly expressed in atherosclerotic plaques and have been implicated in atherogenesis and acute coronary syndromes [17]. Increased MMP-9 expression and activity is

* Corresponding authors. Tel.: +91 40 27193630, +91 40 27191867; fax: +91 40 27193185.
E-mail addresses: giridhar@iict.res.in (S. Kotamraju), narsaiah@iict.res.in, narsaiahbanda84@gmail.com (N. Banda).

0223-5234/$ – see front matter © 2014 Elsevier Masson SAS. All rights reserved.
http://dx.doi.org/10.1016/j.ejmech.2013.12.053

reported in advanced atherosclerotic lesions followed by macrophage infiltration and in progression of atherosclerosis [18]. Macrophage derived MMPs play a potential role in the weakening and ultimate rupture of plaque structure [19]. MMPs have been considered as potential target in many types and stages of cancer and also in the treatment of atherosclerosis.

During the transformation, along with inflammatory property, monocytes acquire a number of specialized functions, including the potential for invasion into sub-endothelial space and also increased phagocytosis activity promoting ingestion of lipid moieties from surroundings and converts to foam cells which ultimately narrows the aortal lumen causing ischemia/stroke. Strategies to prevent monocyte recruitment or/and their transformation into macrophages could attenuate the development of atherogenesis.

Development of hybrids containing two or three biologically active scaffolds possessing good anti-inflammatory and anti-atherogenic activities provide a different biochemical profile. Therefore, there is an urgent need to synthesize hybrid molecules with appreciable biological activity. Benzothiazine derivatives are known to possess versatile biological activities [20,21]. Among them, 1,2-benzothiazine-3-carboxamide-1,1-dioxide derivatives such as piroxicam, ampiroxicam and meloxicam are promising anti-inflammatory agents used worldwide as non-steroidal anti-inflammatory drugs (NSAIDs). Recent findings proved that the 1,2-benzothiazine 1,1-dioxide derivatives as excellent antibacterial, antifungal, anticancer, antioxidant agents and 11β-HSD1 inhibitors. Synthetic modifications of 1,2-benzothiazine 1,1-dioxides to enhance their bio-activity and to develop better anti-inflammatory agents have been intensively studied [22]. In the present work, we have selected 1,2-benzothiazine as a core moiety which was functionalized at 3rd position due to its biological importance of oxime ether link and accomplished a series of novel compounds. Final compounds were screened for anti-inflammatory and their ability to inhibit PMA-induced monocyte-to-macrophage transformation. The promising compounds were further screened for PMA induced MMP-9 gelatinase activity. It was found that compounds **9e** and **9h** significantly inhibited PMA-induced monocyte-to-macrophage transformation and compound **9h**, also greatly inhibited MMP-9 activity.

2. Results and discussion

2.1. Chemistry

The *N*-methyl-3-acetyl-4-hydroxy benzothiazin-1,1-dioxide **4** [23] was prepared starting from sodium salt of saccharin **1**, via *N*-alkylation with α-haloketone to obtain compound **2** followed by ring expansion with sodium ethoxide in ethanol resulted 3-acetyl-4-hydroxy benzothiazin-1,1-dioxide **3**. Compound **3** was further *N*-alkylated using dimethyl sulfate and obtained 3-acetyl-4-hydroxy-2-*N*-methyl benzothiazin-1,1-dioxide **4**. Compound **4** was *O*-alkylated with ethyl iodide to obtain product 1-(4-ethoxy-2-methyl-1,1-dioxo-1,2-dihydro-1λ^6-benzo[*e*][1,2]thiazin-3-yl)ethanone **5** and was further reacted with hydroxylamine hydrochloride in presence of piperidine, as a result the product formed as (*E*)-1-(4-ethoxy-2-methyl-1,1-dioxo-1,2-dihydro-1λ^6-benzo[*e*][1,2] thiazin-3-yl)ethanone oxime **6**. The oxime **6** was reacted with 2-chloro-*N*-substituted acetamide and obtained (*E*)-*N*-substituted-2-(1-(4-ethoxy-2-methyl-1,1-dioxo-1,2-dihydro-1λ^6-benzo[*e*][1,2]thiazin-3-yl)ethylideneaminooxy) acetamide **7**. Alternatively, the 3-acetyl-4-hydroxy-2-*N*-methyl benzothiazin-1,1-dioxide **4** was reacted with hydroxylamine hydrochloride and formed exclusively (*E*)-1-(4-hydroxy-2-*N*-methyl-1,1-dioxo-1,2-dihydro-1λ^6-benzo[*e*][1,2]thiazin-3-yl)ethanone oxime **8**. The oxime **8** was further reacted with 2-chloro-*N*-substituted acetamide and obtained (*E*)-2-(((1-(4-hydroxy-2-methyl-1,1-dioxido-2*H*-benzo[*e*][1,2]thiazin-3-yl)ethylidene) amino)oxy)-*N*-substituted acetamide **9**. The structure of the compound **9e** was established by single crystal X-ray crystallography as shown in Fig. 1 and deposited in data bank as CCDC 952998 (e-mail: deposit@ccdc.cam.ac.uk). The reactions are outlined in Scheme 1.

2.2. Pharmacology

2.2.1. Anti-inflammatory activity

All the final compounds, 1,2-benzothiazine 1,1-dioxide-3-ethanone oxime *N*-aryl acetamide ether derivatives **7a**–**h** and **9a**–**h** were screened for anti-inflammatory activity in the presence of PMA-induced inflammation, by measuring TNF-α, IL-8 and MCP-1 levels using THP-1 monocyte cell system with reference to piroxicam and pioglitazone. It was found that compounds **9e** and **9h** inhibited both TNF-α and MCP-1 activities. Compound **7e** inhibited both IL-8 and MCP-1 activities and compound **9b** inhibited only MCP-1 activity. It is interesting to note that compound **9e** and **9h** showed potent activity against MCP-1 with IC_{50} of 4.0 μM and 2.5 μM respectively. The IC_{50} values of these compounds are much lower than the standard pioglitazone which was found to be 18.6 μM (Table 1). None of the compounds showed a significant effect on viability of cells even at 20 μM concentration as shown in Table 1. This clearly indicates that the anti-inflammatory activities of these compounds are not due to the induction of cytotoxicity in these cells. The structure verses activity data revealed that, the presence of trifluoromethyl group on phenyl ring in combination with presence of hydroxyl on C-4 position appears to be crucial for the observed activity.

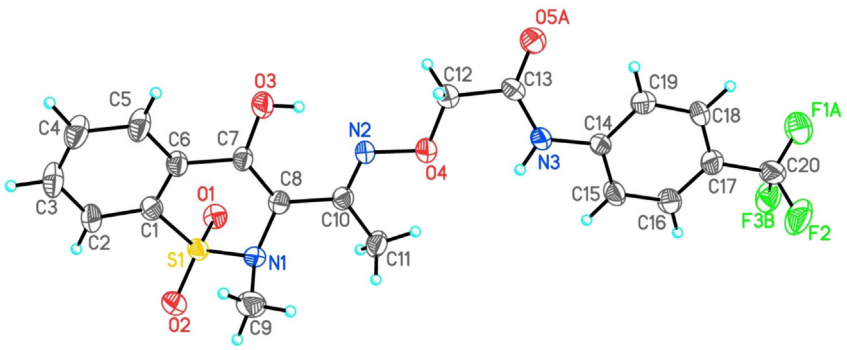

Fig. 1. Crystal structure of compound **9e**. The molecular structure of **9e**, with the atom-numbering scheme: displacement ellipsoids are drawn at the 30% probability level and H atoms are shown as small spheres of arbitrary radius in the ORTEP picture. The crystal structure contains two symmetry independent molecules in the asymmetric unit ($Z' = 2$), however, a single molecule is shown for clarity.

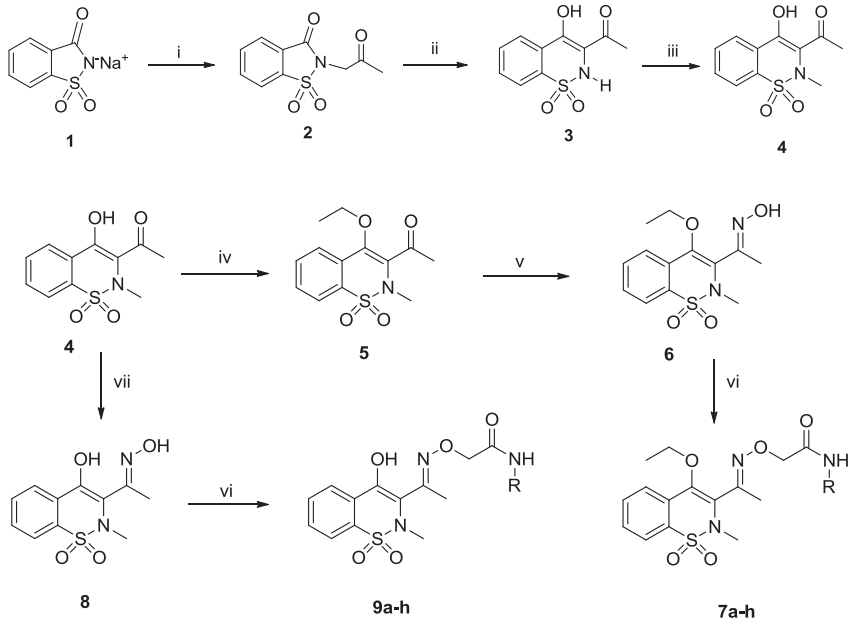

Scheme 1. Preparation of target compounds **7a**–**h** and **9a**–**h**. Reagents and conditions: (i) chloroacetone, DMF, 100 °C, 4 h (ii) NaOEt, RT, 5 min (iii) dimethyl sulfate, 20% aq. NaOH, RT, 30 min (iv) K_2CO_3, Et–I, DMF, 50 °C, 24 h (v) $NH_2OH.HCl$, piperidine, EtOH, reflux, 2 h (vi) K_2CO_3, 2-chloro-*N*-substituted acetamide, dry DMF, 0 °C for 30 min, RT for 12–20 h (vii) $NH_2OH.HCl$, aq NaOH, EtOH, reflux, 2 h.

2.2.2. MMP-9 gelatinase activity

As compounds **9e** and **9h** showed excellent anti-inflammatory activity, we further examined the effects of these compounds on PMA-induced MMP-9 activity during monocyte-to-macrophage transformation by performing in-gel MMP-9 activity assay. For this, THP-1 cells were pretreated with 10 μM concentration of compounds for 2 h followed by PMA stimulation for 48 h. MMP-9 activity was measured in conditioned medium as described in Materials and Methods. It was observed that compound **9h** inhibited MMP-9 activity by 75% (Fig. 2).

Table 1
Secretion inhibition efficacy of the synthesized compounds **7a**–**h** and **9a**–**h** for TNF-α,IL-8 and MCP-1.[a]

S. no	Compound	IC_{50} (μM)[b]			Cell viability[d] (% control)
		TNF-α secretion inhibition efficacy	IL-8 secretion inhibition efficacy	MCP-1 secretion inhibition efficacy	
1	**7a**	NA	NA	NA	93.05 ± 1.09
2	**7b**	NA	NA	NA	91.95 ± 2.09
3	**7c**	NA	NA	NA	96.25 ± 1.22
4	**7d**	NA	NA	NA	94.23 ± 3.25
5	**7e**	NA	16.7 ± 1.9	5.7 ± 1.1	93.00 ± 1.26
6	**7f**	NA	NA	NA	97.50 ± 1.29
7	**7g**	NA	NA	NA	92.34 ± 2.01
8	**7h**	NA	NA	NA	90.25 ± 2.87
9	**9a**	NA	NA	NA	94.12 ± 1.69
10	**9b**	NA	NA	9.4 ± 0.7	95.50 ± 3.11
11	**9c**	NA	NA	NA	92.45 ± 1.65
12	**9d**	NA	NA	NA	97.50 ± 1.73
13	**9e**	12.1 ± 1.1	NA	4.0 ± 1.0	93.00 ± 1.41
14	**9f**	NA	NA	NA	95.12 ± 2.51
15	**9g**	NA	NA	NA	92.15 ± 1.52
16	**9h**	6.0 ± 0.7	NA	2.5 ± 0.9	91.25 ± 1.26
	Piroxicam[c]	NA	NT	NT	–
	Pioglitazone	NT	NT	18.6 ± 2.1	–

[a] THP-1 monocytes are pre-treated with 5, 10 and 20 μM concentrations of the above mentioned benzothiazine derivatives (**7a**–**h** and **9a**–**h**) for 2 h before simulation with 100 nM of phorbol 13-myristate 12-acetate (PMA) to induce inflammation for a period of 48 h. At the end of the treatment, conditioned media was collected and levels of TNF-α, IL-8 and MCP-1 were measured by ELISA as described in the Materials and methods (Section 4.3.3).

[b] IC_{50} values are mean ± SD of three independent experiments.

[c] Piroxicam, a known anti-inflammatory agent was used as a positive control; NA: denotes activity >20 μM; NT: indicates 'not tested'.

[d] THP-1 cell viability with synthesized compounds (20 μM).

2.2.3. Inhibition of PMA-induced monocyte to macrophage transformation

Monocyte-to-macrophage transformation is one of the pre-requisite steps in the progression of atherosclerosis. Transformed monocytes initiate inflammatory responses by secreting various pro-inflammatory cytokines. This in turn, initiates the migration and proliferation of smooth muscle cells and eventually the plaque formation as seen in atherosclerosis. PMA treatment induces a greater degree of THP-1 monocyte differentiation into macrophages as reflected by increased cell adherence and increase in cell size along with increased number of cellular organelles including mitochondria [24], upregulation of scavenger receptors like LOX-1, CD-36 etc, which are involved in foam cell formation by enhancing the uptake of LDL-cholesterol [25]. To this angle, we next examined the effect of these compounds on PMA-induced monocytes-to-macrophage transformation. It was found that, pretreatment of compounds **9e** and **9h** at 10 μM concentration significantly inhibited the PMA-induced increase in cell adherence, cell size, mitochondrial number, LOX-1 and CD-36 expressions in THP-1 cells (Fig. 3). These results confirmed that compound **9e** and **9h**

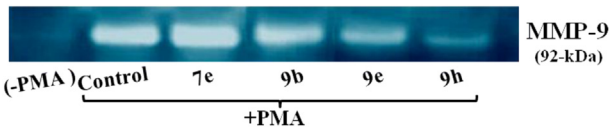

Fig. 2. Compounds **9e** and **9h** inhibit PMA-induced MMP-9 gelatinase activity. Cells were treated with 10 μM concentrations of compounds for 2 h followed by stimulation with PMA for 48 h. MMP-9 activity was performed in conditioned media using gelatin loaded gels.

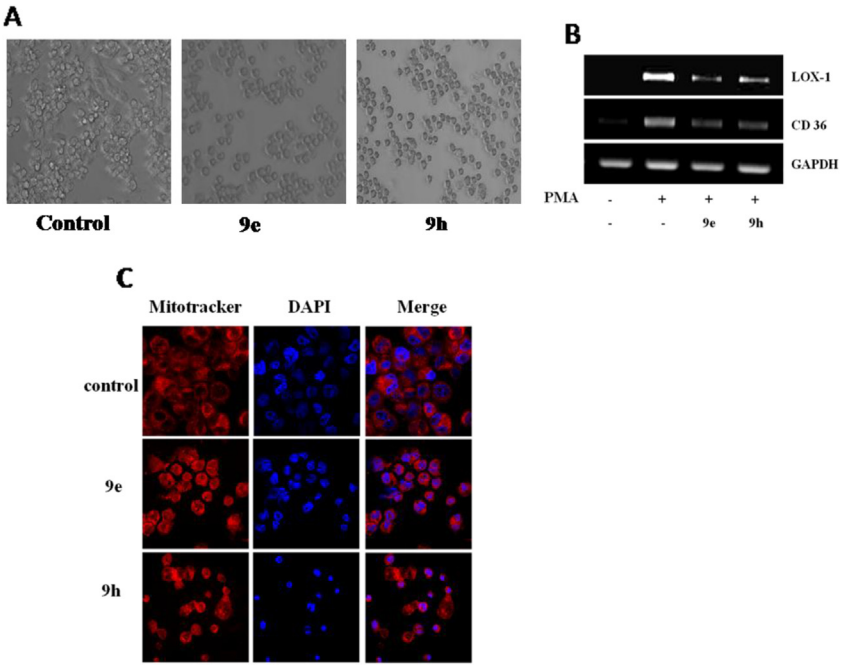

Fig. 3. Compounds **9e** and **9h** inhibit PMA-induced monocyte-to-macrophage transformation. THP-1 cells were pretreated with 10 μM concentrations of compound **9e** and **9h** for 2 h followed by stimulation with PMA (100 nM) for 48 h. A) Shows phase contrast images indicating the inhibition of PMA-induced monocyte transformation by compounds **9e** and **9h**. B) Same as A, except that differentiation markers LOX-1 and CD-36 transcript levels were measured by RT-PCR. C) Same as A, except that mitochondrial staining was performed using mitotracker dye by confocal microscopy.

inhibited PMA-induced monocyte-to-macrophage transformation, a key step during progression of atherogenesis.

3. Conclusion

A series of novel 1,2-benzothiazine 1,1-dioxide-3-ethanone oxime *N*-aryl acetamide ether derivatives were prepared, screened for anti-inflammatory activity *in vitro*. The promising compounds further inhibited MMP-9 gelatinase activity. Compounds **9e** and **9h** even inhibited PMA-induced monocyte-to macrophage-transformation. The structure verses activity data revealed that, the presence of trifluoromethyl group on phenyl ring in combination with presence of hydroxyl on C-4 position appears to be crucial for the observed activity. Therefore, the results of this study suggests that compound **9e** and **9h** can be further studied in-depth in future studies for their vasculo-protective effects.

4. Experimental protocols

4.1. Synthetic chemistry

Melting points were recorded on Casia-Siamia (VMP-AM) melting point apparatus and are uncorrected. IR spectra were recorded on a Perkin–Elmer FT-IR 240-C spectrophotometer using KBr optics. ^{1}H NMR spectra were recorded on Bruker AV 300 MHz and INOVA 500 MHz in $CDCl_3$, ^{13}C NMR spectra were recorded on Bruker AV 75 MHz in $CDCl_3$ & DMSO-d_6 using TMS as an internal standard. All high-resolution spectra were recorded on QSTARXL hybrid MS/MS system (Applied Biosystems, USA) under electro spray ionization. All the reactions were monitored by thin layer chromatography (TLC) on pre-coated silica gel 60 F_{254} (mesh); spots were visualized with UV light. Merck silica gel (60–120 mesh) was used for column chromatography. All the final compounds were analyzed by HPLC to evaluate purity using SHIMADZU LC-20 instrument. Separation was carried out by using a mobile phase of ammonium acetate: acetonitrile (40:60) on Zodiac C_{18} Column (150 mm × 4.6 mm, 5 μM) in an isocratic mode at a flow rate of 1.0 ml/min with Photo-diode Array (PDA) detection at 254 nm and purity exceeded 95%.

4.1.1. Preparation of 1-(4-ethoxy-2-methyl-1,1-dioxido-2H-benzo [e][1,2]thiazin-3-yl)ethanone (**5**)

4.1.1.1. Procedure. The 3-acetyl-4-hydroxy-2-methyl benzothiazin-1,1-dioxide **4** (1.0 g, 4 mmol) and K_2CO_3 (0.83 g, 6 mmol) were taken in dry DMF and stirred at room temperature for 30 min, then iodoethane (0.935 g, 6 mmol) was added. Reaction mixture was heated to 50 °C for 24 h. After completion of reaction, the reaction mixture was poured into ice cold water then solid was filtered, washed with water and dried.

White solid, Yield: 86%; mp: 77–79 °C; I.R. (KBr, cm^{-1}): 1667, 1441, 1335; ^{1}H NMR ($CDCl_3$, 300 MHz): δ 1.40 (t, 3H, $CH_2\underline{CH_3}$, $J = 6.8$ Hz), 2.62 (s, 3H, CH_3), 2.94 (s, 3H, NCH_3), 4.04 (q, 2H, $\underline{CH_2}CH_3$, $J = 6.8$ Hz), 7.66–7.76 (m, 2H, Ar–H), 7.78–7.83 (m, 1H, Ar–H), 7.86–7.91 (m, 1H, Ar–H); MS (ESI, 70 eV): *m/z*: 282 (M + 1).

4.1.2. Preparation of (E)-4-ethoxy-3-(1-(hydroxyimino) ethyl)-2-methyl-2H-benzo[e][1,2] thiazine 1,1-dioxide (**6**)

4.1.2.1. Procedure. The 1-(4-ethoxy-2-methyl-1,1-dioxido-2*H*-benzo[*e*][1,2]thiazin-3-yl)ethanone **5** (1.12 g, 4 mmol) and hydroxylamine hydrochloride (0.55 g, 8 mmol) were taken in ethanol (10 mL) and piperidine (0.4 mL, 4 mmol) was added. The reaction mixture was refluxed for 2 h, and after completion of the reaction, solvent was removed under vacuum. The residue was treated with ice cold water, the separated solid was filtered, washed with water and dried.

White solid, Yield: 83%; mp: 165–167 °C; I.R. (KBr, cm^{-1}): 3290, 1591, 1444, 1345; ^{1}H NMR ($CDCl_3$, 300 MHz): δ 1.27 (t, 3H, $CH_2\underline{CH_3}$, $J = 6.8$ Hz), 2.26 (s, 3H, CH_3), 2.95 (s, 3H, NCH_3), 3.89 (q, 2H, $\underline{CH_2}CH_3$, $J = 6.8$ Hz), 7.56–7.63 (m, 1H, Ar–H), 7.64–7.72 (m, 1H, Ar–H),

7.75–7.80 (m, 1H, Ar–H), 7.83–7.89 (m, 1H, Ar–H), 8.15 (brs, 1H, NH); MS (ESI, 70 eV): *m/z*: 297 (M + 1).

*4.1.3. Preparation of (E)-4-hydroxy-3-(1-(hydroxyimino)ethyl)-2-methyl-2H-benzo[e][1,2] thiazine 1,1-dioxide (**8**)*

4.1.3.1. Procedure. The 3-acetyl-4-hydroxy-2-methyl benzothiazin-1,1-dioxide **4** (1.0 g, 4 mmol) and hydroxylamine hydrochloride (0.55 g, 8 mmol) were taken in ethanol (10 mL) and aq NaOH (0.1 mL, 20%) was added. The reaction mixture was refluxed for 2 h, and after completion of the reaction, solvent was removed under vacuum. The residue was treated with ice cold water and separated solid was filtered, washed with water and dried.

White solid, Yield: 84%; mp: 173–175 °C; I.R. (KBr, cm^{-1}): 3386, 1638, 1547, 1331; ^1H NMR ($CDCl_3$, 300 MHz): δ 2.24 (s, 3H, CH_3), 2.84 (s, 3H, NCH_3), 7.51 (brs, 1H, N–OH), 7.58–7.76 (m, 2H, Ar–H), 7.80–8.00 (m, 2H, Ar–H), 11.84 (brs, 1H, OH); MS (ESI, 70eV): *m/z*: 269 (M + 1).

*4.1.4. Preparation of (E)-2-(((1-(4-ethoxy-2-methyl-1,1-dioxido-2H-benzo[e][1,2]thiazin-3-yl) ethylidene)amino)oxy)-N-substituted acetamide (**7**) and (E)-2-(((1-(4-hydroxy-2-methyl-1,1-dioxido-2H-benzo[e][1,2]thiazin-3-yl)ethylidene)amino) oxy)-N-substituted acetamide (**9**)*

4.1.4.1. General procedure. The oxime **6** or **8** (0.7 mmol) and K_2CO_3 (0.116 g, 0.84 mmol) were taken in dry DMF (5 mL), cooled to 0 °C and stirred for 30 min, then *N*-substituted acetamide (0.77 mmol) was added. The total reaction mixture was stirred at room temperature for 12–20 h. The reaction was monitored by TLC and after completion of the reaction, treated with ice cold water. Aqueous solution was extracted thrice with ethylacetate, combined extracts were washed with water till washings are neutral to pH, dried over anhydrous sodium sulfate and concentrated. The residue was purified by passing through a column packed with silica gel using petroleum ether/EtOAc (8:2) as eluent.

*4.1.4.2. (E)-2-(((1-(4-Ethoxy-2-methyl-1,1-dioxido-2H-benzo[e][1,2] thiazin-3-yl)ethylidene) amino)oxy)-N-phenylacetamide (**7a**).* White solid, Purity: 98.0%; Yield: 80%; mp: 124–126 °C; I.R. (KBr, cm^{-1}): 3363, 1678, 1598, 1534, 1340; ^1H NMR ($CDCl_3$, 500 MHz): δ 1.18 (t, 3H, $CH_2\underline{CH_3}$, J = 6.99 Hz), 2.32 (s, 3H, CH_3), 2.94 (s, 3H, NCH_3), 3.85 (q, 2H, $\underline{CH_2}CH_3$, J = 6.99 Hz), 4.80 (s, 2H, OCH_2), 7.10–7.16 (m, 1H, Ar–H), 7.30–7.37 (m, 2H, Ar–H), 7.53–7.63 (m, 3H, Ar–H), 7.65–7.71 (m, 1H, Ar–H), 7.72–7.76 (m, 1H, Ar–H), 7.82–7.87 (m, 1H, Ar–H), 8.15 (brs, 1H, NH); ^{13}C NMR ($CDCl_3$, 75 MHz): δ 14.7, 15.0, 35.4, 69.3, 73.5, 120.1, 122.8, 124.6, 125.2, 128.3, 128.9, 129.6, 129.9, 132.1, 133.8, 137.0, 144.4, 152.9, 167.4; HRMS *m/z* Calcd. for $C_{21}H_{23}O_5N_3NaS$ ($[M + Na]^+$): 452.1250, found 452.1235.

*4.1.4.3. (E)-2-(((1-(4-Ethoxy-2-methyl-1,1-dioxido-2H-benzo[e][1,2] thiazin-3-yl)ethylidene) amino)oxy)-N-(3-fluorophenyl)acetamide (**7b**).* White solid, Purity: 96.9%; Yield: 76%; mp: 115–117 °C; I.R. (KBr, cm^{-1}): 3356, 1682, 1613, 1533, 1341; ^1H NMR ($CDCl_3$, 300 MHz): δ 1.19 (t, 3H, $CH_2\underline{CH_3}$, J = 6.99 Hz), 2.33 (s, 3H, CH_3), 2.95 (s, 3H, NCH_3), 3.87 (q, 2H, $\underline{CH_2}CH_3$, J = 6.99 Hz), 4.80 (s, 2H, OCH_2), 6.78–6.90 (m, 1H, Ar–H), 7.20–7.34 (m, 2H, Ar–H), 7.47–7.80 (m, 4H, Ar–H), 7.82–7.90 (m, 1H, Ar–H), 8.34 (brs, 1H, NH); ^{13}C NMR ($CDCl_3$, 75 MHz): δ 14.7, 15.0, 35.4, 69.4, 73.5, 107.6 (d, J = 26.3 Hz), 111.3 (d, J = 20.9 Hz), 115.3 (d, J = 2.7 Hz), 123.0, 125.2, 128.3, 129.6, 130.0, 130.1 (d, J = 9.1 Hz), 132.2, 133.9, 138.6 (d, J = 10.9 Hz), 144.5, 153.2, 162.9 (d, J = 245.2 Hz), 167.6; HRMS *m/z* Calcd. for $C_{21}H_{22}O_5N_3FNaS$ ($[M + Na]^+$): 470.1156, found 470.1142.

*4.1.4.4. (E)-2-(((1-(4-Ethoxy-2-methyl-1,1-dioxido-2H-benzo[e][1,2] thiazin-3-yl)ethylidene) amino)oxy)-N-(3-methoxyphenyl)acetamide (**7c**).* White solid, Purity: 96.6%; Yield: 78%; mp: 62–64 °C; I.R. (KBr, cm^{-1}): 3362, 1685, 1609, 1528, 1342; ^1H NMR ($CDCl_3$, 500 MHz): δ 1.20 (t, 3H, $CH_2\underline{CH_3}$, J = 7.02 Hz), 2.33 (s, 3H, CH_3), 2.95 (s, 3H, NCH_3), 3.79 (s, 3H, OCH_3), 3.86 (q, 2H, $\underline{CH_2}CH_3$, J = 7.02 Hz), 4.80 (s, 2H, OCH_2), 6.65–6.71 (m, 1H, Ar–H), 7.03–7.08 (m, 1H, Ar–H), 7.19–7.26 (m, 1H, Ar–H), 7.28–7.35 (m, 1H, Ar–H), 7.57–7.63 (m, 1H, Ar–H), 7.65–7.78 (m, 2H, Ar–H), 7.81–7.87 (m, 1H, Ar–H), 8.25 (brs, 1H, NH); ^{13}C NMR ($CDCl_3$, 75 MHz): δ 14.5, 14.8, 35.1, 54.9, 69.1, 73.2, 105.7, 109.9, 112.0, 122.5, 124.9, 128.2, 129.3, 129.5, 129.7, 131.9, 133.5, 138.1, 144.1, 152.7, 159.7, 167.3; HRMS *m/z* Calcd. for $C_{22}H_{26}O_6N_3S$ ($[M + H]^+$): 460.1537, found 460.1523.

*4.1.4.5. (E)-2-(((1-(4-Ethoxy-2-methyl-1,1-dioxido-2H-benzo[e][1,2] thiazin-3-yl)ethylidene) amino)oxy)-N-(4-methoxyphenyl)acetamide (**7d**).* White solid, Purity: 98.6%; Yield: 70%; mp: 95–97 °C; I.R. (KBr, cm^{-1}): 3368, 1689, 1613, 1529, 1340; ^1H NMR ($CDCl_3$, 500 MHz): δ 1.18 (t, 3H, $CH_2\underline{CH_3}$, J = 7.02 Hz), 2.32 (s, 3H, CH_3), 2.95 (s, 3H, NCH_3), 3.80 (s, 3H, OCH_3), 3.85 (q, 2H, $\underline{CH_2}CH_3$, J = 7.02 Hz), 4.81 (s, 2H, OCH_2), 6.85 (d, 2H, Ar–H, J = 9.00 Hz), 7.47 (d, 2H, Ar–H, J = 8.85 Hz), 7.58–7.64 (m, 1H, Ar–H), 7.67–7.77 (m, 2H, Ar–H), 7.84–7.88 (m, 1H, Ar–H), 8.07 (brs, 1H, NH); ^{13}C NMR ($CDCl_3$, 75 MHz): δ 14.5, 14.8, 35.2, 55.1, 69.2, 73.3, 113.8, 121.9, 122.7, 125.0, 128.2, 129.5, 129.8, 130.0, 132.0, 133.6, 144.1, 152.6, 156.4, 167.2; HRMS *m/z* Calcd. for $C_{22}H_{25}O_6N_3NaS$ ($[M + Na]^+$): 482.1356, found 482.1340.

*4.1.4.6. (E)-2-(((1-(4-Ethoxy-2-methyl-1,1-dioxido-2H-benzo[e][1,2] thiazin-3-yl)ethylidene) amino)oxy)-N-(4-(trifluoromethyl)phenyl) acetamide (**7e**).* White solid, Purity: 96.9%; Yield: 68%; mp: 82–84 °C; I.R. (KBr, cm^{-1}): 3362, 1689, 1612, 1528, 1343; ^1H NMR ($CDCl_3$, 300 MHz): δ 1.20 (t, 3H, $CH_2\underline{CH_3}$, J = 6.80 Hz), 2.34 (s, 3H, CH_3), 2.96 (s, 3H, NCH_3), 3.87 (q, 2H, $\underline{CH_2}CH_3$, J = 6.80 Hz), 4.82 (s, 2H, OCH_2), 7.49–8.09 (m, 8H, Ar–H), 8.54 (brs, 1H, NH); ^{13}C NMR ($CDCl_3$, 75 MHz): δ 14.7, 15.1, 35.5, 69.5, 73.6, 119.8, 123.1, 124.0 (q, J = 271.57 Hz), 125.2, 126.2, 126.5, 128.4, 129.6, 130.1, 132.2, 134.0, 140.3, 144.7, 153.4, 167.9; HRMS *m/z* Calcd. for $C_{22}H_{25}O_6N_3NaS$ ($[M + Na]^+$): 482.1356, found 482.1340.

*4.1.4.7. (E)-N-(3-Chloro-4-fluorophenyl)-2-(((1-(4-ethoxy-2-methyl-1,1-dioxido-2H-benzo[e] [1,2]thiazin-3-yl)ethylidene)amino)oxy) acetamide (**7f**).* White solid, Purity: 98.2%; Yield: 75%; mp: 142–144 °C; I.R. (KBr, cm^{-1}): 3363, 1682, 1608, 1529, 1341; ^1H NMR ($CDCl_3$, 300 MHz): δ 1.19 (t, 3H, $CH_2\underline{CH_3}$, J = 6.80 Hz), 2.31 (s, 3H, CH_3), 2.96 (s, 3H, NCH_3), 3.87 (q, 2H, $\underline{CH_2}CH_3$, J = 6.80 Hz), 4.79 (s, 2H, OCH_2), 7.08–7.17 (m, 1H, Ar–H), 7.45–7.56 (m, 1H, Ar–H), 7.58–7.81 (m, 4H, Ar–H), 7.84–7.92 (m, 1H, Ar–H), 8.40 (brs, 1H, NH); ^{13}C NMR ($CDCl_3$, 75 MHz): δ 14.6, 15.1, 35.4, 69.4, 73.4, 116.6 (d, J = 21.80 Hz), 119.9 (d, J = 7.26 Hz), 121.4 (d, J = 18.16 Hz), 122.4, 123.0, 125.2, 128.4, 129.5, 130.1, 132.2, 133.9, 134.0, 144.5, 153.2, 154.8 (d, J = 247.05 Hz), 167.7; HRMS *m/z* Calcd. for $C_{21}H_{21}O_5N_3ClFNaS$ ($[M + Na]^+$): 504.0766, found 504.0754.

*4.1.4.8. (E)-N-(2,6-Difluorophenyl)-2-(((1-(4-ethoxy-2-methyl-1,1-dioxido-2H-benzo[e][1,2] thiazin-3-yl)ethylidene)amino)oxy)acetamide (**7g**).* White solid, Purity: 97.9%; Yield: 70%; mp: 132–134 °C; I.R. (KBr, cm^{-1}): 3366, 1689, 1611, 1533, 1342; ^1H NMR ($CDCl_3$, 500 MHz): δ 1.16 (t, 3H, $CH_2\underline{CH_3}$, J = 7.02 Hz), 2.31 (s, 3H, CH_3), 2.97 (s, 3H, NCH_3), 3.81 (q, 2H, $\underline{CH_2}CH_3$, J = 7.02 Hz), 4.91 (s, 2H, OCH_2), 6.95–7.03 (m, 2H, Ar–H), 7.20–7.26 (m, 1H, Ar–H), 7.58–7.63 (m, 1H, Ar–H), 7.65–7.75 (m, 2H, Ar–H), 7.83–7.91 (m, 2H, Ar–H&NH); ^{13}C NMR ($CDCl_3$, 75 MHz): δ 14.5, 14.9, 35.3, 69.3, 73.4, 111.7 (dd, J = 19.1 and 3.6 Hz), 113.2 (t, J = 16.35 Hz), 122.9, 125.2, 127.8 (t, J = 9.53 Hz), 128.3, 129.7, 129.9, 132.1, 133.9, 144.2, 152.8, 157.7 (dd, J = 251.5 and 3.6 Hz), 167.9; HRMS *m/z* Calcd. for $C_{21}H_{21}O_5N_3F_2NaS$ ($[M + Na]^+$): 488.1062, found 488.1048.

*4.1.4.9. (E)-N-(4-Chloro-3-(trifluoromethyl)phenyl)-2-(((1-(4-ethoxy-2-methyl-1,1-dioxido-2H-benzo[e][1,2]thiazin-3-yl)ethylidene)amino)oxy)acetamide (**7h**).* White solid, Purity: 98.0%; Yield: 72%; mp: 68–70 °C; I.R. (KBr, cm^{-1}): 3364, 1682, 1610, 1532, 1339; ^1H NMR ($CDCl_3$, 500 MHz): δ 1.16 (t, 3H, $CH_2\underline{CH_3}$, J = 7.02 Hz), 2.31 (s, 3H, CH_3), 2.97 (s, 3H, NCH_3), 3.87 (q, 2H, $\underline{CH_2}CH_3$, J = 7.02 Hz), 4.79 (s, 2H, OCH_2), 7.46–7.51 (m, 1H, Ar–H), 7.60–7.67 (m, 1H, Ar–H), 7.70–7.78 (m, 2H, Ar–H), 7.83–7.90 (m, 2H, Ar–H), 7.95–8.00 (m, 1H, Ar–H), 8.69 (brs, 1H, NH); ^{13}C NMR ($CDCl_3$, 75 MHz): δ 14.6, 14.9, 35.4, 69.3, 73.3, 119.9 (q, J = 5.50 Hz), 122.5 (q, J = 273.4 Hz), 123.0, 124.3, 125.2, 127.0, 128.3, 128.4, 128.7, 130.1, 131.9, 132.3, 133.9, 136.2, 144.4, 153.3, 168.0; HRMS m/z Calcd. for $C_{22}H_{22}O_5N_3ClF_3S$ ($[M + H]^+$): 532.0915, found 532.0904.

*4.1.4.10. (E)-2-(((1-(4-Hydroxy-2-methyl-1,1-dioxido-2H-benzo[e][1,2]thiazin-3-yl)ethylidene) amino) oxy)-N-phenylacetamide (**9a**).* White solid, Purity: 98.2%; Yield: 81%; mp: 150–152 °C; I.R. (KBr, cm^{-1}): 3376, 1702, 1620, 1518, 1344; ^1H NMR ($CDCl_3$, 300 MHz): δ 2.35 (s, 3H, CH_3), 2.84 (s, 3H, NCH_3), 4.75 (s, 2H, OCH_2), 7.09–7.20 (m, 1H, Ar–H), 7.28–7.40 (m, 2H, Ar–H), 7.49–7.74 (m, 4H, Ar–H), 7.78–7.86 (m, 1H, Ar–H), 7.89–7.98 (m, 2H, Ar–H&NH), 11.27 (s, 1H, OH); ^{13}C NMR ($CDCl_3$, 75 MHz): δ 12.2, 39.5, 73.8, 114.6, 120.3, 124.1, 125.0, 126.5, 129.0, 131.2, 132.7, 133.1, 136.5, 150.8, 161.9, 166.3; HRMS m/z Calcd. for $C_{19}H_{19}O_5N_3NaS$ ($[M + Na]^+$): 424.0937, found 424.0928.

*4.1.4.11. (E)-N-(3-Fluorophenyl)-2-(((1-(4-hydroxy-2-methyl-1,1-dioxido-2H-benzo[e][1,2] thiazin-3-yl)ethylidene)amino)oxy)acetamide (**9b**).* White solid, Purity: 96.3%; Yield: 78%; mp: 146–148 °C; I.R. (KBr, cm^{-1}): 3377, 1698, 1618, 1520, 1341; ^1H NMR ($CDCl_3$, 500 MHz): δ 2.37 (s, 3H, CH_3), 2.84 (s, 3H, NCH_3), 4.76 (s, 2H, OCH_2), 6.81–6.90 (m, 1H, Ar–H), 7.16–7.33 (m, 2H, Ar–H), 7.50–7.57 (m, 1H, Ar–H), 7.61–7.75 (m, 2H, Ar–H), 7.81–7.98 (m, 3H, Ar–H&NH), 11.20 (s, 1H, OH); ^{13}C NMR ($CDCl_3$, 75 MHz): δ 12.1, 39.4, 73.7, 107.7 (d, J = 26.4 Hz), 111.6 (d, J = 21.4 Hz), 114.6, 115.5, 124.0, 126.5, 128.9, 130.1 (d, J = 9.3 Hz), 131.2, 132.7, 133.0, 138.1 (d, J = 11.0 Hz), 150.8, 161.9, 162.8 (d, J = 245.4 Hz), 166.5; HRMS m/z Calcd. for $C_{19}H_{18}O_5N_3FNaS$ ($[M + Na]^+$): 442.0843, found 424.0835.

*4.1.4.12. (E)-2-(((1-(4-Hydroxy-2-methyl-1,1-dioxido-2H-benzo[e][1,2]thiazin-3-yl)ethylidene) amino) oxy)-N-(3-methoxyphenyl)acetamide (**9c**).* White solid, Purity: 96.1%; Yield: 76%; mp: 64–66 °C; I.R. (KBr, cm^{-1}): 3378, 1702, 1622, 1524, 1340; ^1H NMR ($CDCl_3$, 300 MHz): δ 2.36 (s, 3H, CH_3), 2.85 (s, 3H, NCH_3), 3.82 (s, 3H, OCH_3), 4.75 (s, 2H, OCH_2), 6.62–6.77 (m, 1H, Ar–H), 6.94–7.35 (m, 4H, Ar–H), 7.57–7.75 (m, 2H, Ar–H), 7.80–7.98 (m, 2H, Ar–H&NH), 11.25 (s, 1H, OH); ^{13}C NMR ($CDCl_3$, 75 MHz): δ 12.7, 39.5, 55.3, 73.8, 106.1, 110.7, 112.4, 114.7, 124.1, 126.4, 129.0, 129.7, 131.2, 132.7, 133.1, 137.8, 150.7, 160.1, 161.7, 166.3; HRMS m/z Calcd. for $C_{20}H_{21}O_6N_3NaS$ ($[M + Na]^+$): 454.1043, found 454.1032.

*4.1.4.13. (E)-2-(((1-(4-Hydroxy-2-methyl-1,1-dioxido-2H-benzo[e][1,2]thiazin-3-yl)ethylidene) amino)oxy)-N-(4-methoxyphenyl)acetamide (**9d**).* White solid, Purity: 99.2%; Yield: 72%; mp: 190–192 °C; I.R. (KBr, cm^{-1}): 3383, 1694, 1620, 1519, 1341; ^1H NMR ($CDCl_3$, 500 MHz): δ 2.36 (s, 3H, CH_3), 2.84 (s, 3H, NCH_3), 3.80 (s, 3H, OCH_3), 4.76 (s, 2H, OCH_2), 6.88 (d, 2H, Ar–H, J = 8.85 Hz), 7.45 (d, 2H, Ar–H, J = 9.00 Hz), 7.62–7.74 (m, 2H, Ar–H), 7.78 (brs, 1H, NH), 7.82–7.87 (m, 1H, Ar–H), 7.92–7.97 (m, 1H, Ar–H), 11.28 (s, 1H, OH); ^{13}C NMR (DMSO-d_6, 75 MHz): δ 11.6, 38.6, 54.8, 73.1, 113.5, 115.0, 121.3, 123.4, 125.7, 128.6, 131.0, 131.1, 132.4, 132.7, 148.5, 155.5, 158.7, 166.0; HRMS m/z Calcd. for $C_{20}H_{21}O_6N_3NaS$ ($[M + Na]^+$): 454.1043, found 454.1040.

*4.1.4.14. (E)-2-(((1-(4-Hydroxy-2-methyl-1,1-dioxido-2H-benzo[e][1,2]thiazin-3-yl)ethylidene) amino)oxy)-N-(4-(trifluoromethyl) phenyl)acetamide (**9e**).* White solid, Purity: 99.3%; Yield: 69%; mp: 166–168 °C; I.R. (KBr, cm^{-1}): 3378, 1698, 1618, 1524, 1342; ^1H NMR ($CDCl_3$, 300 MHz): δ 2.37 (s, 3H, CH_3), 2.85 (s, 3H, NCH_3), 4.77 (s, 2H, OCH_2), 7.57–7.75 (m, 6H, Ar–H), 7.82–7.87 (m, 1H, Ar–H), 7.91–7.96 (m, 1H, Ar–H), 8.02 (brs, 1H, NH), 11.21 (s, 1H, OH); ^{13}C NMR ($CDCl_3$, 75 MHz): δ 12.1, 39.4, 73.6, 114.6, 119.9, 123.8 (q, J = 272.2 Hz), 124.0, 126.1 (q, J = 4.4 Hz), 126.2, 126.4, 128.8, 131.3, 132.7, 132.9, 139.7, 150.8, 161.9, 166.7; HRMS m/z Calcd. for $C_{20}H_{18}O_5N_3F_3NaS$ ($[M + Na]^+$): 492.0811, found 492.0809.

*4.1.4.15. (E)-N-(3-Chloro-4-fluorophenyl)-2-(((1-(4-hydroxy-2-methyl-1,1-dioxido-2H-benzo[e] [1,2]thiazin-3-yl)ethylidene)amino) oxy)acetamide (**9f**).* White solid, Purity: 99.4%; Yield: 74%; mp: 154–156 °C; I.R. (KBr, cm^{-1}): 3382, 1696, 1621, 1520, 1339; ^1H NMR ($CDCl_3$, 300 MHz): δ 2.34 (s, 3H, CH_3), 2.86 (s, 3H, NCH_3), 4.74 (s, 2H, OCH_2), 7.11 (t, 1H, Ar–H, J = 8.68 Hz), 7.34–7.42 (m, 1H, Ar–H), 7.60–7.79 (m, 3H, Ar–H), 7.81–7.88 (m, 2H, Ar–H & NH), 7.91–7.97 (m, 1H, Ar–H), 11.21 (s, 1H, OH); ^{13}C NMR (DMSO-d_6, 75 MHz): δ 11.1, 38.3, 72.5, 114.2, 115.4 (d, J = 22.00 Hz), 119.1, 119.3, 119.4, 121.3, 122.9, 125.3, 128.2, 130.1, 131.8, 132.0, 134.0, 148.7, 153.3 (d, J = 245.38 Hz), 159.2, 166.1; HRMS m/z Calcd. for $C_{19}H_{17}O_5N_3ClFNaS$ ($[M + Na]^+$): 476.0453, found 476.0456.

*4.1.4.16. (E)-N-(2,6-Difluorophenyl)-2-(((1-(4-hydroxy-2-methyl-1,1-dioxido-2H-benzo[e][1,2] thiazin-3-yl)ethylidene)amino)oxy) acetamide (**9g**).* White solid, Purity: 96.3%; Yield: 70%; mp: 178–180 °C; I.R. (KBr, cm^{-1}): 3384, 1694, 1620, 1528, 1340; ^1H NMR ($CDCl_3$, 300 MHz): δ 2.36 (s, 3H, CH_3), 2.85 (s, 3H, NCH_3), 4.86 (s, 2H, OCH_2), 6.92–7.04 (m, 2H, Ar–H), 7.19–7.29 (m, 1H, Ar–H), 7.49 (brs, 1H, NH), 7.60–7.76 (m, 2H, Ar–H), 7.81–7.88 (m, 1H, Ar–H), 7.94–8.03 (m, 1H, Ar–H), 11.20 (s, 1H, OH); ^{13}C NMR (DMSO-d_6, 75 MHz): δ 11.3, 38.4, 72.3, 110.8 (d, J = 22.56 Hz), 112.9 (t, J = 16.50 Hz), 114.2, 123.0, 125.5, 127.1 (t, J = 9.35 Hz), 128.4, 130.2, 131.9, 132.1, 148.8, 157.3 (dd, J = 250.9 and 4.9 Hz), 159.7, 166.8; HRMS m/z Calcd. for $C_{19}H_{17}O_5N_3F_2NaS$ ($[M + Na]^+$): 460.0749, found 460.0735.

*4.1.4.17. (E)-N-(4-Chloro-3-(trifluoromethyl)phenyl)-2-(((1-(4-hydroxy-2-methyl-1,1-dioxido-2H-benzo[e][1,2]thiazin-3-yl)ethylidene)amino)oxy)acetamide (**9h**).* White solid, Purity: 98.3%; Yield: 72%; mp: 132–134 °C; I.R. (KBr, cm^{-1}): 3386, 1698, 1618, 1526, 1342; ^1H NMR ($CDCl_3$, 500 MHz): δ 2.37 (s, 3H, CH_3), 2.85 (s, 3H, NCH_3), 4.78 (s, 2H, OCH_2), 7.47–7.50 (m, 1H, Ar–H), 7.63–7.68 (m, 1H, Ar–H), 7.70–7.74 (m, 1H, Ar–H), 7.77–7.80 (m, 1H, Ar–H), 7.84–7.86 (m, 1H, Ar–H), 7.90–7.98 (m, 3H, Ar–H&NH), 11.20 (s, 1H, Ar–H); ^{13}C NMR ($CDCl_3$, 75 MHz): δ 12.3, 39.5, 73.6, 114.6, 119.3 (q, J = 5.4 Hz), 122.4 (q, J = 273.4 Hz), 124.1, 124.3, 126.5, 127.6, 128.6, 128.8, 131.3, 132.0, 132.8, 133.0, 135.5, 151.0, 162.2, 166.7; HRMS m/z Calcd. for $C_{20}H_{18}O_5N_3ClF_3S$ ($[M + H]^+$): 504.0602, found 504.0596.

4.2. Crystal structure of compound **9e**

In addition to the spectral characterization, a single crystal of compound **9e** is developed from methanol/water (80:20). X-ray data for the compound were collected at room temperature using a Bruker Smart Apex CCD diffractometer with graphite monochromated Mo-Kα radiation (λ = 0.71073 Å) with ω-scan method [26]. Preliminary lattice parameters and orientation matrices were obtained from four sets of frames. Unit cell dimensions were determined using 3910 reflections for compound **9e** data. Integration and scaling of the intensity data was accomplished using SAINT program [26]. The structures were solved by Direct Methods using SHELXS97 [27] and refinement was carried out by full-matrix least-squares technique using SHELXL97 [27]. Anisotropic displacement

parameters were included for all non-hydrogen atoms. All H atoms were positioned geometrically and treated as riding on their parent C atoms, with C–H distances of 0.93–0.97 Å, and with $U_{iso}(H) = 1.2U_{eq}$ (C) or $1.5U_{eq}$ for methyl atoms. Two fluorine atoms of $-CF_3$ group in the first symmetry independent molecule were disordered over two sites [F1A(0.53) & F1B(0.47); F3A(0.52) & F3B(0.48)]. Similarly, a single fluorine atom of $-CF_3$ group in the second symmetry independent molecule was disordered over two sites [F6A(0.56) & F6B(0.44)]. PART and ISOR instructions were used for disorder modeling of the fluorine atoms and DFIX was used for restraining all the C–F bond distances to 1.295 Å with e.s.d 0.002 in the crystal structure refinement.

Crystal data for **9e**: $C_{20}H_{18}F_3N_3O_5S$, $M = 469.43$, colorless needle, 0.28 × 0.14 × 0.09 mm^3, monoclinic, space group *Pn* (No. 7), $a = 7.7781(9)$, $b = 27.127(3)$, $c = 10.1351(11)$ Å, $\beta = 99.674(2)^\circ$, $V = 2108.1(4)$ $Å^3$, $Z = 4$, $D_c = 1.479$ g/cm^3, $F_{000} = 968$, CCD area detector, Mo-Kα radiation, $\lambda = 0.71073$ Å, $T = 293(2)$K, $2\theta_{max} = 50.0^\circ$, 20,239 reflections collected, 7409 unique ($R_{int} = 0.0369$), Final *GooF* = 1.058, $R_1 = 0.0709$, $wR_2 = 0.1732$, *R* indices based on 5665 reflections with $I > 2\sigma(I)$ (refinement on F^2), 619 parameters, 60 restraints, $\mu = 0.218$ mm^{-1}. CCDC 952998 contains the supplementary crystallographic data. The data can be obtained free of charge at www.ccdc.cam.ac.uk/conts/retrieving.html [or from the Cambridge Crystallographic Data Centre (CCDC), 12 Union Road, Cambridge CB2 1EZ, UK; fax: +44(0) 1223 336 033; email: deposit@ccdc.cam.ac.uk].

4.3. Biological experiments

4.3.1. THP-1 cell culture

THP-1 monocytes were obtained from ATCC and grown in RPMI 1640 (Sigma) containing 10% FBS (Lonza), non essential amino acids, penicillin (100 U/mL), and streptomycin (100 μg/mL) in 75-cm^2 filter vent flasks (Costar), incubated at 37 °C in a humidified atmosphere containing 5% CO_2 and 95% air.

4.3.2. Measurement of cell viability

The effect of synthesized compounds on cell viability was determined by Trypan blue dye exclusion assay. THP-1 cells were seeded at a density of 2×10^5 cells/ml in 24-well plates in triplicates and were treated with compounds (20 μM) for 72 h. At the end of the treatments, cells were harvested and re-suspended in 0.4% Trypan blue (Invitrogen) and cell viability percentage was counted using cell countess chamber (Invitrogen).

4.3.3. Enzyme-linked immunosorbent assay for TNF-α, IL-8 and MCP-1 inhibition

To check the inhibitory effects of 1,2-benzothiazine 1,1-dioxide-3-ethanone oxime *N*-aryl acetamide ether derivatives (**7a**–**h** and **9a**–**h**) on PMA-induced inhibition of inflammation, THP-1 monocytes were seeded at a density of 2×10^5/ml in 24 well plates. Cells were pre-treated with 5, 10 and 20 μM concentrations of compounds for 2 h before they were stimulated with 100 nM of PMA. After 48 h of PMA stimulation supernatants were harvested and assayed for TNF-α, IL-8 and 72 h for MCP-1 estimation using an enzyme-linked immunosorbent assay (ELISA) kit following the manufacturer's instructions (eBiosciences, San Diego, CA, USA). The absorbance in each well was measured with a microplate reader at 450 nm and corrected at 570 nm. Concentrations of cytokines released were obtained and the percentage of inhibition of cytokines production was calculated as compared to control conditions. IC_{50} was also obtained as a mean of anti-inflammatory potency, expressing the predicted concentration of the correspondent compound able to reach 50% inhibition. The standard curves were calculated by plotting the pg/ml concentrations *versus* absorbance values from the standards, and were used to quantify the amount of cytokines released by the cells.

4.3.4. Gelatin zymography

THP-1 monocytes were seeded in 24 well plates for studying MMP-9 activity by gelatin zymography. Cells were pretreated for 2 h with 10 μM concentrations of compounds **9e** and **9h** followed by stimulation with 100 nm PMA. After 48 h of treatment, 25 μl of conditioned media was mixed with 25 μl of Laemmli buffer without β-mercaptoethanol and ran the 10% SDS-PAGE containing 0.1% gelatin. The gel was incubated in Zymogram renaturing Buffer (0.25% Triton X-100 solution) with gentle agitation for 30 min at room temperature and allowed to develop using Zymogram developing buffer (50 mM Tris base, 50 mM Tris–HCl, 0.2 mM NaCl, 5 mM $CaCl_2$ and 0.02% Brij 35) at room temperature for overnight. Gels were stained with Coomassie Blue R-250 solution to get clear bands against a dark blue background where the protease had digested the substrate.

4.3.5. Qualitative analysis of monocyte/macrophage transformation by light microscopy

THP-1 cells were pretreated with 10 μM concentration of compounds **9e** and **9h** for 2 h followed by PMA stimulation. After 48 h, medium was removed, washed twice with warm DPBS and phase contrast pictures were taken by light microscopy to study the monocyte/macrophage adherence and transformation.

4.3.6. Measurement of mitochondrial biogenesis by confocal microscopy

THP-1 monocytes were pretreated with 10 μM concentration of compounds **9e** and **9h** for 2 h in cover glass bottom dishes (SPL life science) and stimulated with 100 nM PMA. After 48 h, media was removed and incubated in 1 mL of HBSS (Hanks balanced salt solution) containing 200 nM mitotracker solution CMXROS (molecular probes) for 1 h followed by counter staining of nucleus with DAPI (sigma). Images were taken using an Olympus confocal microscope equipped with Rhodamine and DAPI filter settings. Data are representative of five different fields of view. After every step, cells were washed with gentle shaking for 5 min at very low RPM speed to prevent the loss of weakly adherent cells.

4.3.7. Measurement of LOX-1, CD-36 gene expression levels by RT-PCR

THP-1 monocytes were pretreated for 2 h with 10 μM of **9e** and **9h** compounds followed by stimulation with 100 nM of PMA for a period of 36 h. At the end of the treatment, cells were collected in TRIzol (sigma), to extract total RNA. Subsequently, cDNA was prepared using Fermentas cDNA synthesis kit. LOX-1 and CD-36 expressions were measured by RT-PCR using respective gene specific primers. GAPDH was used as a loading control. The primers sequences used are given in Table 2.

Table 2
The sequences of LOX-1, CD-36 primers.

Gene	Primer	Sequence	Product size (bp)
LOX-1	Forward	ACTCTCCATGGTGGTGCCTGG	252
	Reverse	CATTCAGCTTCCGAGCAAGGG	
CD-36	Forward	TGCAAAACGGCTGCAGGTCAA	394
	Reverse	GAGGATGACAGGAATGCAGGGC	
GAPDH	Forward	GCACCACCAACTGCTTAGCAC	516
	Reverse	CCCTGTTGCTGTAGCCAAAT	

Acknowledgments

Authors are thankful to the Council of Scientific & Industrial Research, New Delhi, India for the financial support through XII five year plan projects DITSF code: CSC-0204 and "Small Molecules in Lead Exploration" (SMiLE). Authors (GMR, PN, RNR and SBV) are also thankful to Council of Scientific and Industrial Research (CSIR), India for providing financial assistance in the form of Research Fellowship and contingency grant.

Appendix A. Supplementary data

Supplementary data related to this article can be found at http://dx.doi.org/10.1016/j.ejmech.2013.12.053.

References

[1] G.S. Hotamisligil, P. Arner, J.F. Caro, R.L. Atkinson, B.M.J. Spiegelman, Increased adipose tissue expression of tumor necrosis factor-alpha in human obesity and insulin resistance, J. Clin. Invest. 95 (1995) 2409–2415.
[2] H.G. Rus, F. Niculescu, R. Vlaicu, Tumor necrosis factor-alpha in human arterial wall with atherosclerosis, Atherosclerosis 89 (1991) 247–254.
[3] K. Selmaj, C.S. Raine, B. Cannella, C.F.J. Brosnan, Identification of lymphotoxin and tumor necrosis factor in multiple sclerosis lesions, J. Clin. Invest. 87 (1991) 949–954.
[4] R.C. Newton, C.P. Decicco, Therapeutic potential and strategies for inhibiting tumor necrosis factor-alpha, J. Med. Chem. 42 (1999) 2295–2314.
[5] F. Lovering, Y. Zhang, Therapeutic potential of TACE inhibitors in stroke, Curr. Drug Targets CNS Neurol. Disord. 4 (2005) 161–168.
[6] J. Such, D.J. Hillebrand, C. Guarner, L. Berk, P. Zapater, J. Westengard, C. Peralta, G. Soriano, J. Pappas, B.A. Runyon, Tumor necrosis factor-alpha, interleukin-6, and nitric oxide in sterile ascitic fluid and serum from patients with cirrhosis who subsequently develop ascitic fluid infection, Dig. Dis. Sci. 46 (2001) 2360–2366.
[7] S.B. Desai, D.E. Furst, Problems encountered during anti-tumour necrosis factor therapy, Best Pract. Res. Clin. Rheumatol. 20 (2006) 757–790.
[8] F. Shen, S.J. Chen, X.J. Dong, H. Zhong, Y.T. Li, G.F. Cheng, Suppression of IL-8 gene transcription by resveratrol in phorbol ester treated human monocytic cells, J. Asian Nat. Prod. Res. 5 (2003) 151–157.
[9] F.W. Luscinskas, R.E. Gerszten, E.A. Garcia-Zepeda, Y.C. Lim, M. Yoshida, H.A. Ding, M.A. Gimbrone Jr., A.D. Luster, A. Rosenzweig, C–C and C–X–C chemokines trigger firm adhesion of monocytes to vascular endothelium under flow conditions, Ann. N. Y. Acad. Sci. 902 (2000) 288–293.
[10] P.G. Jorens, J.B. Richman-Eisenstat, B.P. Housset, P.D. Graf, I.F. Ueki, J. Olesch, J.A. Nadel, Interleukin-8 induces neutrophil accumulation but not protease secretion in the canine trachea, Am. J. Physiol. 263 (1992) 708–713.
[11] B. Gesser, M. Lund, N. Lohse, C. Vestergaad, K. Matsushima, S. Sindet-Pedersen, S.L. Jensen, K. Thestrup-Pedersen, C.G. Larsen, IL-8 induces T cell chemotaxis, suppresses IL-4, and up-regulates IL-8 production by CD4+ T cells, J. Leukocyte Biol. 59 (1996) 407–411.
[12] K. Hayashida, T. NankiT, H. Girschick, S. Yavuz, T. Ochi, P.E. Lipsky, Synovial stromal cells from rheumatoid arthritis patients attract monocytes by producing MCP-1 and IL-8, Arthritis Res. 3 (2001) 118–126.
[13] P. Sartipy, D.J. Loskutoff, Monocyte chemoattractant protein 1 in obesity and insulin resistance, Proc. Natl. Acad. Sci. U. S. A. 100 (2003) 7265–7270.
[14] A. Sahinarslan, S.A. Kocaman, S. Topal, U. Erçin, N. Bukan, T. Timurkaynak, The relation of serum monocyte chemoattractant protein-1 level with coronary atherosclerotic burden and collateral degree in stable coronary artery disease, Turk. Kardiyol. Dern. Ars. 39 (2011) 269–275.
[15] T.C. Dawson, W.A. Kuziel, T.A. Osahar, N. Maeda, Absence of CC chemokine receptor-2 reduces atherosclerosis in apolipoprotein E-deficient mice, Atherosclerosis 143 (1999) 205–211.
[16] C. Gialeli, A.D. Theocharis, N.K. Karamanos, Roles of matrix metalloproteinases in cancer progression and their pharmacological targeting, FEBS J. 278 (2011) 16–27.
[17] C.B. Jones, D.C. Sane, D.M. Herrington, Matrix metalloproteinases: a review of their structure and role in acute coronary syndrome, Cardiovasc. Res. 59 (2003) 812–823.
[18] D. Wagsater, C. Zhu, J. Bjorkegren, J. Skogsberg, P. Eriksson, MMP-2 and MMP-9 are prominent matrix metalloproteinases during atherosclerosis development in the Ldlr(−/−) Apob(100/100) mouse, Int. J. Mol. Med. 28 (2011) 247–253.
[19] W.J. Kim, E.M. Bae, Y.J. Kang, H.U. Bae, S.H. Hong, J.Y. Lee, J.E. Park, B.S. Kwon, K. Suk, W.H. Lee, Glucocorticoid-induced tumour necrosis factor receptor family related protein (GITR) mediates inflammatory activation of macrophages that can destabilize atherosclerotic plaques, Immunology 119 (2006) 421–429.
[20] (a) S. Sabatini, F. Gosetto, S. Serritella, G. Manfroni, O. Tabarrini, N. Iraci, J.P. Brincat, E. Carosati, M. Villarini, G.W. Kaatz, V. Cecchetti, Pyrazolo[4,3-*c*][1,2]benzothiazines 5,5-dioxide: a promising new class of *Staphylococcus aureus* NorA efflux pump inhibitors, J. Med. Chem. 55 (2012) 3568–3572;
(b) M. Zia-ur-Rehman, J.A. Choudary, M.R. Elsegood, H.L. Siddiqui, K.M. Khan, A facile synthesis of novel biologically active 4-hydroxy-*N*′-(benzylidene)-2*H*-benzo[*e*][1,2]thiazine-3-carbohydrazide 1,1-dioxides, Eur. J. Med. Chem. 44 (2009) 1311–1316;
(c) N. Ahmad, M. Zia-ur-Rehman, H.L. Siddiqui, M.F. Ullah, M. Parvez, Microwave assisted synthesis and structure-activity relationship of 4-hydroxy-*N*′-[1-phenylethylidene]-2*H*/2-methyl-1,2-benzothiazine-3-carbohydrazide 1,1-dioxides as anti-microbial agents, Eur. J. Med. Chem. 46 (2011) 2368–2377.
[21] (a) S.H. Kim, R. Ramu, S.W. Kwon, S.H. Lee, C.H. Kim, S.K. Kang, S.D. Rhee, M.A. Bae, S.H. Ahn, D.C. Ha, H.G. Cheon, K.Y. Kim, J.H. Ahn, Discovery of cyclicsulfonamide derivatives as 11 beta-hydroxysteroid dehydrogenase 1 inhibitors, Bioorg. Med. Chem. Lett. 20 (2010) 1065–1069;
(b) S.H. Kim, S.W. Kwon, S.Y. Chu, J.H. Lee, B. Narsaiah, C.H. Kim, S.K. Kang, N.S. Kang, S.D. Rhee, M.A. Bae, S.H. Ahn, D.C. Ha, K.Y. Kim, J.H. Ahn, Identification of cyclicsulfonamide derivatives with an acetamide group as 11β-hydroxysteroid dehydrogenase 1 inhibitors, Chem. Pharm. Bull. 59 (2011) 46–52.
[22] (a) E.S. Lazer, C.K. Miao, C.L. Cywin, R. Sorcek, H.C. Wong, Z. Meng, I. Potocki, M. Hoermann, R.J. Snow, M.A. Tschantz, T.A. Kelly, D.W. McNeil, S.J. Coutts, L. Churchill, A.G. Graham, E. David, P.M. Grob, W. Engel, H. Meier, G. Trummlitz, Effect of structural modification of enol-carboxamide-type nonsteroidal antiinflammatory drugs on COX-2/COX-1 selectivity, J. Med. Chem. 40 (1997) 980–989;
(b) M. El-Kemary, M. Gil, A. Douhal, Relaxation dynamics of piroxicam structures within human serum albumin protein, J. Med. Chem. 50 (2007) 2896–2902.
[23] M. Ahmad, H.L. Siddiqui, M. Zia-ur-Rehman, M. Parvez, Anti-oxidant and anti-bacterial activities of novel *N*′-arylmethylidene-2-(3,4-dimethyl-5,5-dioxido-pyrazolo[4,3-*c*][1,2] benzothiazin-2(4*H*)-yl) acetohydrazides, Eur. J. Med. Chem. 45 (2010) 698–704.
[24] M. Daigneault, J.A. Preston, H.M. Marriott, M.K. Whyte, D.H. Dockrell, The identification of markers of macrophage differentiation in PMA-stimulated THP-1 cells and monocyte-derived macrophages, PLoS One 5 (2010) e8668.
[25] A. Eguchi, Y. Kaneko, A. Murakami, H. Ohigashi, Zerumbone suppresses phorbol ester-induced expression of multiple scavenger receptor genes in THP-1 human monocytic cells, Biosci. Biotechnol. Biochem. 71 (2007) 935–945.
[26] SMART & SAINT, Software Reference Manuals. Versions 6.28a & 5.625, Bruker Analytical X-ray Systems Inc., Madison, Wisconsin, U.S.A, 2001.
[27] Sheldrick, G.M. SHELXS97 and SHELXL97, Programs for Crystal Structure Solution and Refinement; University of Gottingen: Germany, 19.